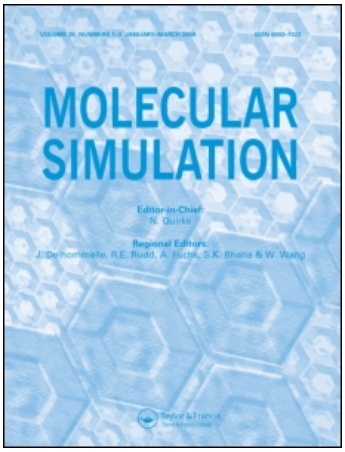

Molecular Simulation
Publication details, including instructions for authors and subscription information:
http://www.informaworld.com/smpp/title~content=t713644482

Homology modelling and molecular dynamics study of human fatty acid amide hydrolase

Yong-Shan Zhao[a]; Qing-Chuan Zheng[a]; Hong-Xing Zhang[a]; Hui-Ying Chu[a]; Chia-Chung Sun[a]
[a] State Key Laboratory of Theoretical and Computational Chemistry, Institute of Theoretical Chemistry, Jilin University, Changchun, PR China

To cite this Article Zhao, Yong-Shan , Zheng, Qing-Chuan , Zhang, Hong-Xing , Chu, Hui-Ying and Sun, Chia-Chung(2009) 'Homology modelling and molecular dynamics study of human fatty acid amide hydrolase', Molecular Simulation, 35: 14, 1201 — 1208
To link to this Article: DOI: 10.1080/08927020903033133
URL: http://dx.doi.org/10.1080/08927020903033133

Molecular Simulation
Vol. 35, No. 14, December 2009, 1201–1208

Taylor & Francis
Taylor & Francis Group

Homology modelling and molecular dynamics study of human fatty acid amide hydrolase

Yong-Shan Zhao, Qing-Chuan Zheng, Hong-Xing Zhang*, Hui-Ying Chu and Chia-Chung Sun

State Key Laboratory of Theoretical and Computational Chemistry, Institute of Theoretical Chemistry, Jilin University, Changchun 130023, PR China

(*Received 28 February 2009; final version received 6 May 2009*)

The three-dimensional (3D) model of the human fatty acid amide hydrolase (hFAAH) was constructed based on the crystal structure of the rat FAAH (PDB code 1MT5) in complex with a substrate using Modeller9v2 program. With the aid of molecular mechanics and molecular dynamics method, the last model was obtained and further assessed by Profile-3D, Prosa2003 and Procheck, which confirms that the refined model is reliable. Furthermore, the docking results of propofol and its structural analogue into the active site of hFAAH indicate that 2,6-di-sec-butyl phenol is a more preferred ligand than others, which is in good agreement with the experimental results. From the docking studies, we also suggest that Phe192, Ile238, Thr377, Leu380, Phe381, Phe388 and Leu404 in the hFAAH are seven important determinant residues in binding as they have strong van der Waal interactions with the ligand.

Keywords: fatty acid amide hydrolase; docking; homology modelling

1. Introduction

Fatty acid amide hydrolase (FAAH) [1,2] is responsible for the hydrolysis of the fatty acid amide class of lipid transmitters which belong to the amidase signature family [3]. FAAH is of particular importance due to the intriguing biological activities of its substrates that include the endogenous cannabinoid N-arachidonoyl ethanolamine (anandamide, AEA) [4–7], sleep-inducing agent oleamide [8–10], anorexigenic agent N-oleoyl ethanolamide [11] and anti-inflammatory agent N-palmitoyl ethanolamide [12]. Studies of FAAH inactivation suggest that this enzyme could be an attractive target for the treatment of pain [13–15], inflammation [16] or sleep disorders [17].

Despite the therapeutic potential of FAAH in various diseases, only a few potent and selective inhibitors have been identified. Until recently, FAAH inhibitors with greatly improved selectivity have been described [18–20]. In 2008, Mileni et al. [21] reported a humanised rat FAAH protein which exhibits the inhibitor sensitivity profiles of the human FAAH. However, no report has been found about the three-dimensional (3D) structure of the human fatty acid amide hydrolase (hFAAH), which has seriously hampered further determination of biological roles and structure-based design of potent and selective inhibitors of hFAAH. Thus, knowledge of the 3D structure is essential for understanding the relationship of enzyme function and structure, and theoretical studies on the binding mode of the hFAAH with its inhibitors are necessary to reveal the interaction occurring in the active site.

To our best knowledge, the homology modelling is an efficient method for the 3D structure construction of proteins [22–24]. In this paper, we first tried to obtain a reliable 3D structure of the hFAAH based on rat FAAH (PDB code 1MT5) [25] by the homology modelling method, followed by molecular mechanics (MM) and molecular dynamics (MD) simulation to refine the initial model. The quality of the resulting substrate-free 3D model of hFAAH was critically assessed via geometric and energetic assessments. Subsequently, the model structure was then used to search the active site and carry out binding studies by flexible docking with 2,6-diisopropyl phenol (propofol) and its structural analogues. Finally, according to the analysis, in the docked complexes, certain key residues responsible for the substrate specificity were identified. The results might be a good starting point for further determination of the biological role and structure-based inhibitor design of the hFAAH.

2. Theory and methods

2.1 Homology modelling

The primary sequence of hFAAH (accession No. O00519) was obtained from the SWISS-PROT and TrEMBL database of the ExPASy Molecular Biology Server [26]. The first step was to search for a number of related sequences to find a related protein as a template by the BLAST program [27] (http://www.ncbi.nih.gov), and then the sequence alignment was performed by ClustalW program (version 1.83) [28] using a gap penalty of 10 and employing BLOSUM30 weight matrix. Program Modeller9v2 [29] was performed to build the 3D structure of hFAAH. Modeller is an implementation of an

*Corresponding author. Email: zhanghx@mail.jlu.edu.cn

ISSN 0892-7022 print/ISSN 1029-0435 online

DOI: 10.1080/08927020903033133
http://www.informaworld.com

automated approach to comparative modelling by satisfaction of spatial restraints [30,31]. Within Modeller9v2, the sequence alignment was used to generate several models and the outcomes were ranked on the basis of the internal scoring function of the program. The model with the highest score was validated by the probability density functions and chosen for further refinement.

2.2 MD simulation

The tleap module in Amber10 [32] was used to generate an all-atom model of the hFAAH on the basis of the initial model, and then the protein was solvated in a rectangular box of about 16,614 water molecules. The TIP3P model [33] was used and the water box extended 9 Å away from any solute atom.

Prior to the MD simulation, a series of minimisations were performed. All water molecules were first minimised while restraining the protein-atomic positions with a harmonic potential. The system was then energy-minimised without restraints for 2000 steps using a combination of the steepest descent and conjugated gradient methods. After the system was gradually heated from 10 to 300 K over 20 ps using the NVT ensemble, the MD simulation was carried out to examine the quality of the model structures by checking their stability via performing a 1 ns simulation at 1 atm and 300 K with the NPT ensemble. During the simulation, all bonds involving hydrogen atoms were constrained using the SHAKE algorithm [34]. The time step of the simulations was 2.0 fs with a cut-off of 10 Å for the non-bonded interaction. Coordinates were saved every 0.5 ps during the entire process. The ff99SB all-atom Amber force field [35] was used as the protein.

The lowest energy structure during the 1 ns simulation was calculated. After removing the water molecules, the lowest energy structure was submitted for energy minimisation with a conjugate gradient method for 3000 steps. In this step, the quality of the initial model was improved.

2.3 Model quality assessment

After the optimisation procedure, the final 3D model of hFAAH was checked using Profile-3D [36], Procheck [37] and Prosa2003 [38]. The Profile-3D method measured the compatibility of an amino acid sequence with a known 3D protein structure. Procheck was employed for geometric evaluations and Prosa2003 was used to evaluate the quality of consistency between the native fold and the sequence and to examine the energy of residue–residue interactions, respectively.

2.4 Binding-site analysis

The binding-site module [39] is a suite of programs in Insight II for identifying and characterising protein-active sites, binding sites and functional residues from protein structures and multiple sequence alignments. In this study, ActiveSite-Search was used to identify protein-active sites and binding sites by locating a cavity in the hFAAH structure. When the search was completed, the largest site was automatically displayed on the structure. Moreover, the other sites were also obtained by using Asite-Display. The results can be used to guide the protein-ligand docking experiment.

2.5 Docking inhibitors to hFAAH

Affinity, which uses a combination of the Monte Carlo type and simulated annealing procedure to dock, is a suite of programs for automatically docking a ligand (guest) to a receptor (host) [40]. By means of the 3D structure of propofol and its structural analogues that were obtained from the Gaussian03 program [41], the automated molecular docking was performed using docking program affinity. A key feature is that the 'bulk' of the receptor, defined as the atoms that are not in the binding-site specified, is held rigid during the docking process, while the binding-site atoms and ligand atoms are movable. The potential function of the complex was assigned by using the consistent-valence force field and the cell multiple approach was used for non-bonding interactions. To account for the solvent effect, the centred enzyme–ligand complex was solvated in layers of TIP3P water molecules with 5 Å. Finally, the docked complex of hFAAH with propofol and its structural analogues was selected by the criteria of interacting energy combined with the geometrical matching quality. The complex was used as the starting conformation for further energetic minimisation and geometrical optimisation before the final model was generated. The global structure with the lowest energy was chosen for computing the intermolecular binding energies. The Ludi [42] program was used to characterise the affinity and the binding preference of a ligand to the protein.

3. Results and discussion

3.1 Homology modelling of hFAAH

A high level of sequence identity should guarantee a more accurate alignment between the target sequence and template structure. In the result of the BLAST search, the high-sequence identity between the hFAAH and 1MT5 is 84%, which allows for a rather straightforward sequence alignment (Figure 1). These residues may be important for the binding of inhibitors. The automated homology model building was performed using protein structure modelling program Modeller9v2. The best-ranked model was chosen based on probability density functions. With this procedure, the initial model was complete. This model was refined by MM optimisation and MD simulation, and

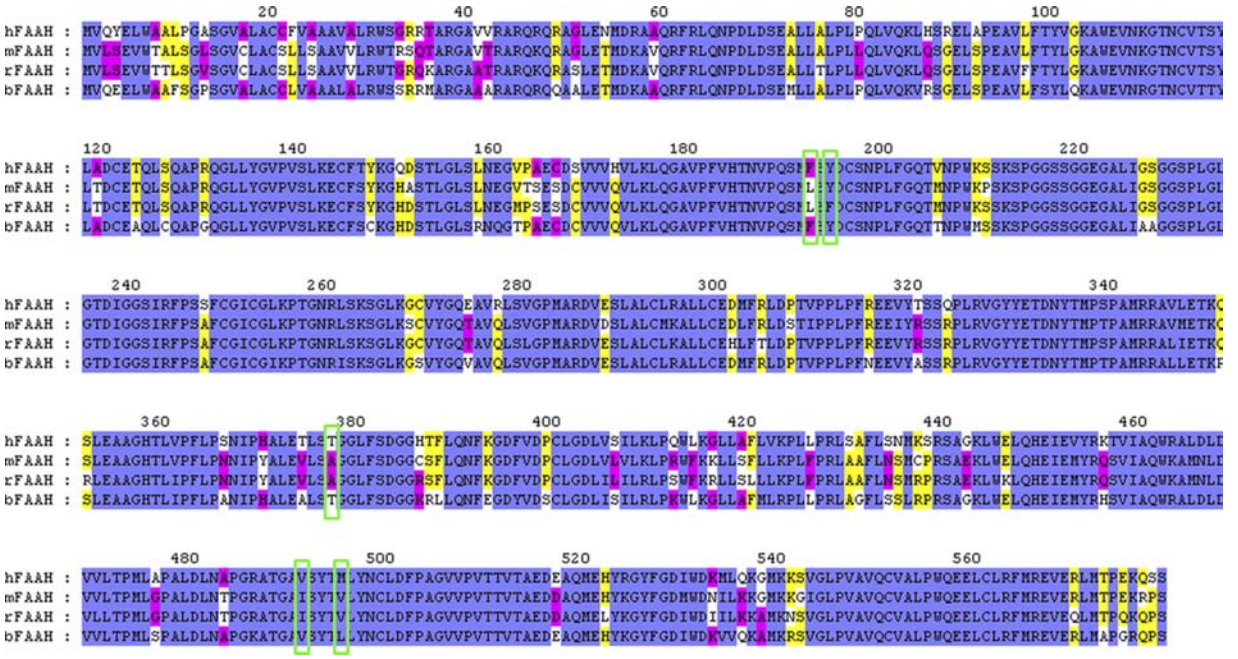

Figure 1. Sequence alignment of hFAAH and 1MT5. The important residues in the active site are highlighted with violet rectangles.

then the final stable structure of hFAAH was obtained as displayed in Figure 2(a). From Figure 2(a), we can see that this enzyme has 16 helices and 10 sheets.

The conformation with the lowest energy was chosen and the 3D structure was superimposed with 1MT5. Their root-mean-square deviation (RMSD) value is 1.17 Å (Figure 2(b)), indicating a good overall structure alignment with 1MT5. The final structure with the lowest energy was checked by Profile-3D (Figure 3) and the self-compatibility score for this protein is 262.9, which is higher than the expected score 248.3. Note that the compatibility scores above 0 correspond to the 'acceptable' side chain environment. From Figure 3, we can see that all residues are reasonable. Then, the structure of the hFAAH was evaluated using Procheck and Prosa2003. The *z*-score and overall score of Procheck geometric assessment are −9.82 and −0.94, respectively, which indicate that the homology model is very reliable. The majority of the residues of the hFAAH model are found to occupy the most favoured regions in the Ramachandran plot. The percentage of $\Phi-\Psi$ angles in the allowed Ramachandran regions is 99.8% in the hFAAH model.

Figures 4(a,b) display the total energy and RMSD of the heavy atoms compared with the starting coordinates during the 1 ns of MD. It is important to monitor the total energy and the RMSD variations in order to determine whether and when the equilibration is reached. As seen from Figures 4(a,b), the total energy and RMSD remain

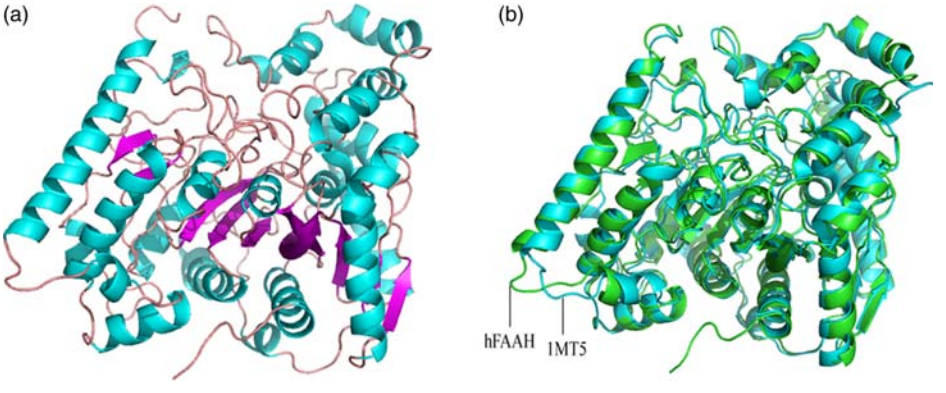

Figure 2. (a) The final 3D-structure of hFAAH. The α-helix is represented by blue colour, the β-sheet is represented by pink colour and the loops are represented by brown colour. (b) Comparison of the refined hFAAH model with its template 1MT5. The white ribbon is a representation of the hFAAH. The red ribbon is a representation of 1MT5.

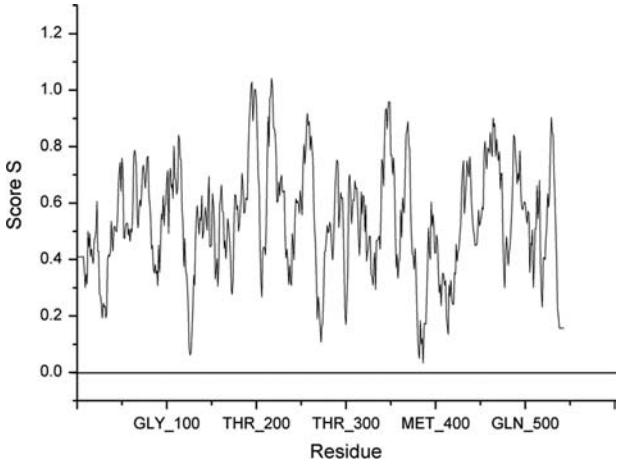

Figure 3. The 3D profiles verified results of the hFAAH model, residues with positive compatibility score are reasonably folded.

constant after 800 ps time, indicating that the 3D model of hFAAH is stable and can be used for subsequent docking calculation.

3.2 Identification of binding-site in hFAAH

In order to investigate the interaction between hFAAH and the ligand, the binding pocket was defined as a subset that contains residues in which the atoms are within 5 Å of the ligand. The active sites were obtained using a binding-site module. It was reported that the FAAH is a member of a large class of enzymes termed the amidase signature class, which uses an unusual Ser–Ser–Lys catalytic triad to hydrolyse amide bonds on a wide range of small-molecular substrates [25]. In hFAAH, the active site is formed by a hydrophobic tunnel, leading from the membrane-bound surface to the hydrophilic catalytic triad (Ser241, Ser217 and Lys142). It is obvious that the chosen site is in good agreement with the conclusion drawn by Mileni et al. [21]. This site is composed of 23 residues (Phe192-Tyr194, Ile238-Gly239, Ser241, Thr377-Phe381, Phe388, Leu401, Leu404, Ile407-Leu408, Leu429, Phe432, Asn435-Met436, Thr488-Gly489, Val491 and Met495). According to the sequence comparisons and the structure of 1MT5 [25], six of these amino acids in the active site were identified, which differed between rFAAH (L192, F194, A377, S435, I491 and V495) and hFAAH (F192, Y194, T377, N435, V491 and M495) [21]. Based on the experiment and our theoretical predicted results, this site was chosen as the more favourable binding site to dock the ligand.

3.3 Docking study

Many different classes of FAAH inhibitors have been available in the past decade, including various fatty acid

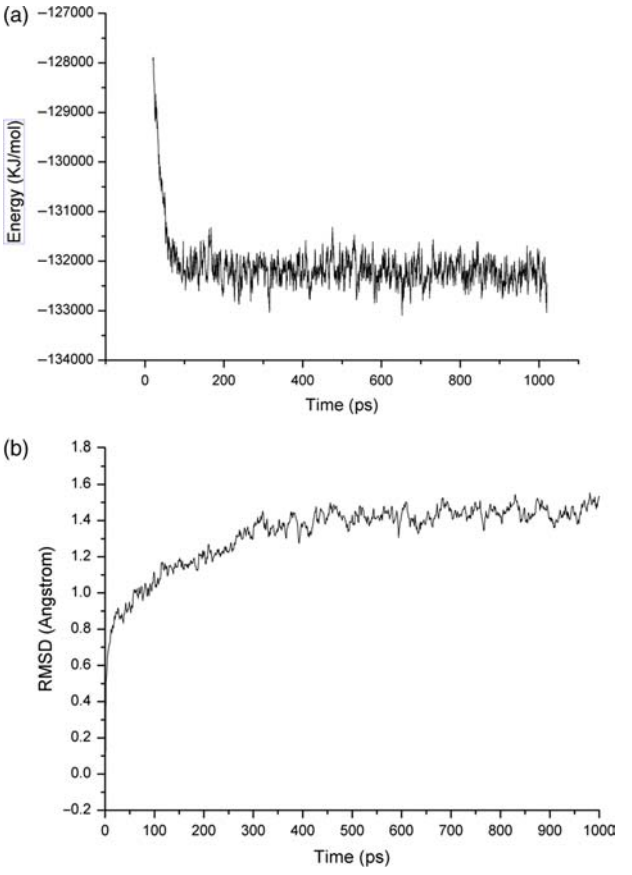

Figure 4. (a) Total energy and (b) RMSD with respect to simulation time for a 1 ns free MD simulation on the hFAAH model.

derivatives [43–47] and non-lipid inhibitors such as α-keto heterocycles [19,48], carbamate derivatives [49,50] and most recently piperidine/piperazine ureas [20]. However, some hFAAH inhibitors have been shown to be less selective and potent *in vivo*. Interestingly, the currently marketed analgesics and anaesthetics may have already derived some of their efficacy from the FAAH inhibition. The anaesthetic agent propofol is identified as a potential competitive FAAH inhibitor with an IC_{50} value of 14 μM in rat brain membranes; mice anaesthetised with 100 mg/kg propofol showed significant elevations in the brain AEA compared with mice anaesthetised with 60 mg/kg thiopental, a much weaker FAAH inhibitor ($IC_{50} = 2$ mM) [51]. In the following discussion, the interactions of the ligands with the receptor in the modelled complexes are investigated, and we shall compare the inhibition ability of the hFAAH by propofol with that of its structural analogues. These complexes will reveal how inhibitors achieve potency and specificity for hFAAH, thus offering key insights into guiding future drug design efforts. The 3D structures of propofol and its structural analogues are shown in Figure 5.

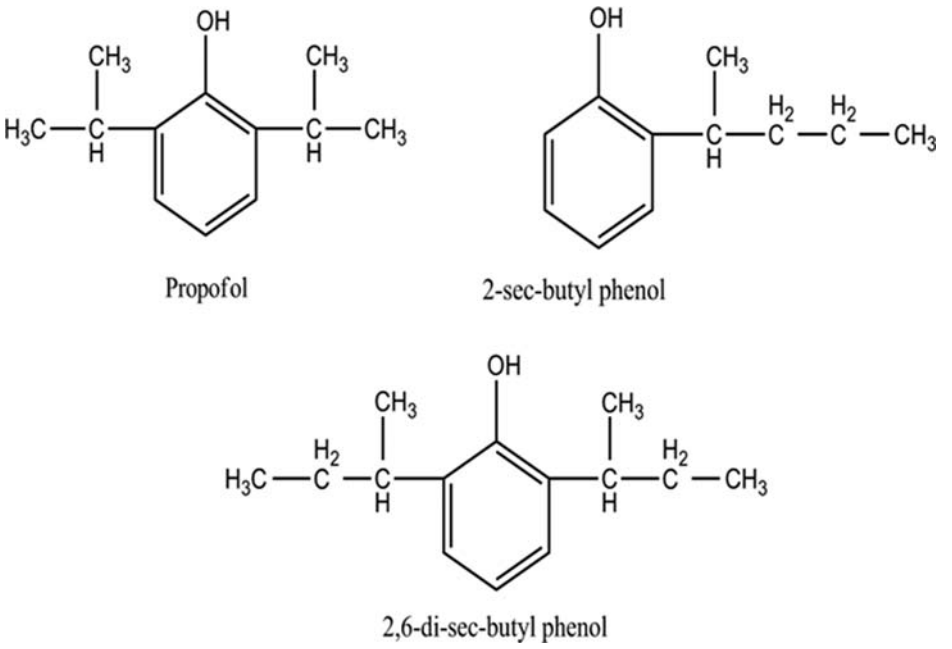

Figure 5. The structures of propofol and its structural analogues.

To understand the interaction between hFAAH and propofol, a propofol–hFAAH complex was generated by the affinity module and the binding 3D conformation of the complex as described in Figure 6(a). In order to determine the key residues that comprise the active site of the model, the interaction energies of the substrate with each of the residues in the active site were calculated. Significant binding-site residues in the models were identified by the total interaction energy between the ligand and each amino acid residues in the enzyme. This identification, compared with a definition based on the distance from the ligands, can clearly show the relative significance for every residue. Table 1 gives the interaction energies including the total, van der Waals and electrostatic energies with the total energies lower than $-1.0\,\text{kcal mol}^{-1}$.

As seen from Table 1, the enzyme–substrate complex has a favourable total interaction energy which is $-35.81\,\text{kcal mol}^{-1}$; the van der Waals and electrostatic energies are -34.55 and $-1.26\,\text{kcal mol}^{-1}$, respectively. These results indicate that an attractive interaction is important. Through the interaction analysis, we get to know that Phe192, Ile238, Gly239, Ser241, Thr377, Leu380, Phe381, Phe388, Leu401, Leu404, Thr488, Gly489, Val491 and Met495 are important anchoring residues for propofol and mainly contribute to the substrate interaction. For most of the hydrophobic residues of the active site such as Phe192, Ile238, Leu380, Phe381, Phe388 and Leu404, the interaction energies between hFAAH and propofol are mainly contributed by the van der Waals interactions, which is in good agreement with the experimental result by Seierstad and Breitenbucher

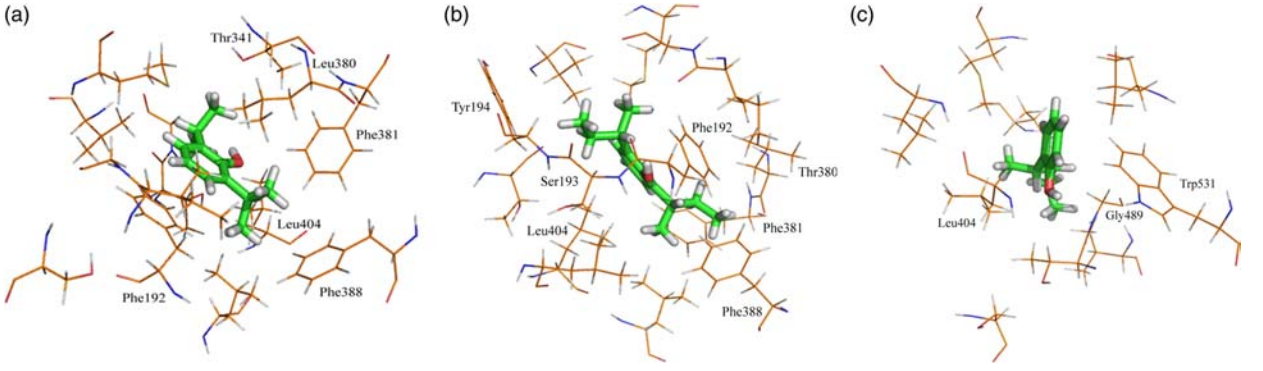

Figure 6. A close view of the binding of hFAAH with (a) propofol (b) 2,6-di-sec-butyl phenol (c) 2-sec-butyl phenol. The ligands and residues are represented by sticks and lines, respectively.

Table 1. The total energy (E_{total}), van der Waals energy (E_{vdw}) and electrostatic energy (E_{ele}) between individual residues of hFAAH and 2,6-diisopropyl phenol (kcal mol^{-1}).

	Propofol (2,6-diisopropyl phenol)		
Residue	E_{vdw}	E_{ele}	E_{total}
Total	−34.55	−1.26	−35.81
Phe192	−9.29	0.66	−8.63
Ile238	−2.66	−0.09	−2.75
Gly239	−1.20	0.04	−1.06
Ser241	−1.46	−0.04	−1.50
Thr377	−1.41	−0.01	−1.42
Leu380	−4.26	−0.24	−4.30
Phe381	−3.27	−0.24	−3.51
Phe388	−1.92	−0.11	−2.03
Leu401	−1.07	−0.01	−1.08
Leu404	−2.28	−0.22	−2.50
Thr488	−1.60	−0.26	−1.86
Gly489	−1.62	−0.32	−1.94
Val491	−1.28	0.14	−1.14
Met495	−1.26	0.14	−1.12

[52]. Furthermore all the residues mentioned above are conserved from the alignment result in this subfamily except Phe192, Thr377 and Phe388. Thus, we can conjecture that the residues Phe192, Ile238, Thr377, Leu380, Phe381, Phe388 and Leu404 are important determinant residues in binding as they have strong van der Waals contacts with propofol.

Patel et al. [51] reported that the structural analogues of propofol are the potential and selective hFAAH inhibitors and the presence and size of the substitutions at positions 2 and 6 of propofol are critical determinants of potency. The binding model of 2,6-di-sec-butyl phenol with hFAAH is shown in Figure 6(b). To determine the key residues that comprise the active site of the model, the interaction energies of the substrate with each of the residues in the active site were calculated. Table 2 gives the interaction energies including the total, van der Waals and electrostatic energies with the total energies lower than −1.0 kcal mol^{-1}.

Table 2. The total energy (E_{total}), van der Waals energy (E_{vdw}) and electrostatic energy (E_{ele}) between individual residues of hFAAH and 2,6-di-sec-butyl phenol (kcal mol^{-1}).

	2,6-di-sec-butyl phenol		
Residue	E_{vdw}	E_{ele}	E_{total}
Total	−35.85	−3.04	−38.89
Phe192	−8.14	−1.24	−9.38
Ser193	−1.67	−0.21	−1.88
Tyr194	−2.35	−0.50	−2.85
Ile238	−0.81	−0.31	−1.11
Gly239	−1.01	−0.15	−1.16
Thr380	−2.29	−0.20	−2.49
Phe381	−4.57	0.01	−4.56
Phe388	−3.80	−0.01	−3.81
Leu401	−1.06	0.01	−1.05
Leu404	−3.93	−0.28	−4.21
Lue408	−1.22	−0.05	−1.27
Thr488	−1.33	−0.27	−1.60
Val491	−2.48	0.01	−2.47
Met495	−1.19	0.06	−1.13

Table 3. The total energy (E_{total}), van der Waals energy (E_{vdw}) and electrostatic energy (E_{ele}) between individual residues of hFAAH and 2-sec-butyl phenol (kcal mol^{-1}).

	2-sec-butyl phenol		
Residue	E_{vdw}	E_{ele}	E_{total}
Total	−25.53	0.01	−25.52
Phe193	−2.01	−0.06	−2.07
Thr377	−2.34	0.22	−2.12
Leu404	−4.65	−0.59	−5.24
Ile408	−2.00	0.04	−1.96
Leu429	−2.46	−0.05	−2.51
Met436	−1.90	−0.15	−2.05
Thr488	−2.62	0.27	−2.35
Gly489	−3.18	0.43	−2.75
Val491	−1.00	−0.08	−1.08
Trp531	−3.37	−0.02	−3.39

The interaction energy between hFAAH and 2,6-di-sec-butyl phenol is −38.89 kcal mol^{-1}, which is higher compared with the hFAAH–propofol complex. Except for some important hydrophobic residues of the active site mentioned above, another two important residues Ser193 and Tyr194 have a large contribution to the interaction between hFAAH and 2,6-di-sec-butyl phenol.

The 3D conformation of the 2-sec-butyl phenol bound with hFAAH is shown in Figure 6(c). The van der Waals energies of 2-sec-butyl phenol with hFAAH dramatically decrease due to the loss of the interactions between some important hydrophobic residues and hFAAH. The interaction energy between the inhibitor and the important residues of hFAAH is listed in Table 3.

For the docked structures, the interaction energies' order is 2,6-di-sec-butyl phenol > propofol > 2-sec-butyl phenol. For the Ludi scores, the interaction energies' order is 2,6-di-sec-butyl phenol > propofol > 2-sec-butyl phenol (Table 4). These results qualitatively validate the modelling and docking studies described for this subfamily.

In summary, the analysis of interactions between all three ligands and hFAAH reveals the fact that van der Waals energy has a larger contribution to ligand binding than the electrostatic energy. This is in line with the fact that the binding pocket of hFAAH is mainly composed of hydrophobic residues. Furthermore, there are many common and important residues in the hFAAH binding to 2-sec-butyl phenol, propofol and 2,6-di-sec-butyl phenol. Among these ligands, the total energy between hFAAH and 2,6-di-sec-butyl phenol is the highest, whereas the total energy between hFAAH and 2-sec-butyl phenol is the lowest. Compared with 2,6-di-sec-butyl phenol and

Table 4. The interaction energies (kcal mol^{-1}) between the ligands and hFAAH.

Substrate	E_{vdw} (kcal mol^{-1})	E_{ele} (kcal mol^{-1})	E_{total} (kcal mol^{-1})	Ludi score	IC_{50} (μM)
Propofol	−34.55	−1.26	−35.81	357	52
2,6-di-sec-butyl phenol	−35.85	−3.04	−38.89	397	9
2-sec-butyl phenol	−25.53	0.01	−25.52	343	35

2-sec-butyl phenol, they have the same main moiety, but the only difference is that there exists a large butyl moiety in 2,6-di-sec-butyl phenol. They both can have strong van der Waals interactions with hFAAH, whereas the large butyl moiety in 2,6-di-sec-butyl phenol is a strong attractive group and can induce the conformational changes in the active site residues of hFAAH and make the binding of 2,6-di-sec-butyl phenol with hFAAH more energy favourable. In the case of 2-sec-butyl phenol, it essentially has poor interactions with hFAAH, mainly because it lacks a butyl moiety at two positions of phenol and loosely binds to the enzyme, not well fixed in the substrate-binding pocket of the active site. Thus, this explains why the complex of 2-sec-butyl phenol and hFAAH has a lower interaction. The results are in good agreement with the experiment reported by Patel et al. [51].

4. Conclusions

The 3D structure of hFAAH had not been known. In this investigation, the 3D structure of hFAAH was built by the homology modelling that was based on the known crystal structure of rat FAAH (PDB code 1MT5). Moreover, energy minimisation and MD simulation were used to refine the structure. With this model, a flexible docking study was performed and the docking results indicate that the presence and size of substitutions at positions 2 and 6 are critical determinants of potency. Phe192, Ile238, Thr377, Leu380, Phe381, Phe388 and Leu404 may be the key amino acid residues interacting with the ligands, and Ser193 and Tyr194 may help 2,6-di-sec-butyl phenol interact with hFAAH steadily. These results will offer further experimental studies of structure–function relationships.

Acknowledgements

This work is supported by the Natural Science Foundation of China, Key Projects in the National Science & Technology Pillar Program, and Specialised Research Fund for the Doctoral Program of Higher Education (Grant Nos 20573042, 2006BAE03B01 and 20070183046)

References

[1] B.F. Cravatt, D.K. Giang, S.P. Mayfield, D.L. Boger, R.A. Lerner, and N.B. Gilula, *Molecular characterization of an enzyme that degrades neuromodulatory fatty-acid amides*, Nature 384 (1996), pp. 83–87.

[2] D.K. Giang and B.F. Cravatt, *Molecular characterization of human and mouse fatty acid amide hydrolases*, Proc. Natl Acad. Sci. USA 4 (1997), pp. 2238–2242.

[3] H. Chebrou, F. Bigey, A. Arnaud, and P. Galzy, *Study of the amidase signature group*, Biochim. Biophys. Acta 1298 (1996), pp. 285–293.

[4] W.A. Devane, L. Hanus, A. Breuer, R.G. Pertwee, L.A. Stevenson, G. Griffin, D. Gibson, A. Mandelbaum, A. Etinger, and R. Mechoulam, *Isolation and structure of a brain constituent that binds to the cannabinoid receptor*, Science 258 (1992), pp. 1946–1949.

[5] B.R. Martin, R. Mechoulam, and R.K. Razdan, *Discovery and characterization of endogenous cannabinoids*, Life Sci. 65 (1999), pp. 573–595.

[6] V. Di Marzo, T. Bisogno, L. De Petrocellis, D. Melck, and B.R. Martin, *Cannabimimetic fatty acid derivatives: the anandamide family and other 'Endocannabinoids'*, Curr. Med. Chem. 6 (1999), pp. 721–744.

[7] H.H. Schmid, P.C. Schmid, and V. Natarajan, *N-acylated glycerophospholipids and their derivatives*, Prog. Lipid. Res. 29 (1990), pp. 1–43.

[8] D.L. Boger, S.J. Henriksen, and B.F. Cravatt, *Oleamide: an endogenoussleep-inducing lipid and prototypical member of a new class of lipid signaling molecules*, Curr. Pharm. Des. 4 (1998), pp. 303–314.

[9] B.F. Cravatt, R.A. Lerner, and D.L. Boger, *Structure determination of an endogenous sleep-inducing lipid* cis-*9-octadecenamide (Oleamide): a synthetic approach to the chemical analysis of trace quantities of a natural product*, J. Am. Chem. Soc. 118 (1996), pp. 580–590.

[10] B.F. Cravatt, O. Prospero-Garcia, G. Suizdak, N.B. Gilula, S.J. Henriksen, D.L. Boger, and R.A. Lerner, *Chemical characterization of a family of brain lipids that induce sleep*, Science 268 (1995), pp. 1506–1509.

[11] D.M. Lambert, S. Vandevoorde, K.O. Jonsson, and C.J. Fowler, *The palmitoylethanolamide family: a new class of antiinflammatory agents?* Curr. Med. Chem. 9 (2002), pp. 663–674.

[12] F. Rodríguez de Fonseca, M. Navarro, R. Gómez, L. Escuredo, F. Nava, J. Fu, E. Murillo-Rodríguez, A. Giuffrida, J. LoVerme, S. Gaetani, S. Kathuria, C. Gall, and D. Piomelli, *An anorexic lipid mediator regulated by feeding*, Nature 414 (2001), pp. 209–212.

[13] B.F. Cravatt, K. Demarest, M.P. Patricelli, M.H. Bracey, D.K. Giang, B.R. Martin, and A.H. Lichtman, *Supersensitivity to anandamide and enhanced endogenous cannabinoid signaling in mice lacking fatty acid amide hydrolase*, Proc. Natl Acad. Sci. USA 98 (2001), pp. 9371–9376.

[14] A.H. Lichtman, C.C. Shelton, T. Advani, and B.F. Cravatt, *Mice lacking fatty acid amide hydrolase exhibit a cannabinoid receptor-mediated phenotypic hypoalgesia*, Pain 109 (2004), pp. 319–327.

[15] B.F. Cravatt, A. Saghatelian, E.G. Hawkins, A.B. Clement, M.H. Bracey, and A.H. Lichtman, *Functional disassociation of the central and peripheral fatty acid amide signaling systems*, Proc. Natl Acad. Sci. USA 101 (2004), pp. 10821–10826.

[16] M. Karsak, E. Gaffal, R. Date, L. Wang-Eckhardt, J. Rehnelt, S. Petrosino, K. Starowicz, R. Steuder, E. Schlicker, B.F. Cravatt, R. Mechoulam, R. Buettner, S. Werner, V. Di Marzo, T. Tüting, and A. Zimmer, *Attenuation of allergic contact dermatitis through the endocannabinoid system*, Science 316 (2007), pp. 1494–1497.

[17] (a) S. Huitroń-Reseńdiz, L. Gombart, B.F. Cravatt, and S.J. Henriksen, *Effect of oleamide on sleep and its relationship to blood pressure, body temperature, and locomotor activity in rats*, Exp. Neurol. 172 (2001), pp. 235–243. (b) S. Huitroń-Reseńdiz, M. Sanchez-Alavez, D.N. Wills, B.F. Cravatt, S.J. Henriksen,

Characterization of the sleep–wake patterns in mice lacking fatty acid amide hydrolase, Sleep 27 (2004), pp. 857–865.
[18] D. Leung, C. Hardouin, D.L. Boger, and B.F. Cravatt, *Discovering potent and selective reversible inhibitors of enzymes in complex proteomes*, Nat. Biotechnol. 21 (2003), pp. 687–691.
[19] D.L. Boger, S. Haruhiko, E.L. Aaron, P.H. Michael, A.F. Robert, M. Hiroshi, D.W. Gordon, J.A. Bryce, P.P. Matthew, and F.C. Benjamin, *Exceptionally potent inhibitors of fatty acid amide hydrolase: the enzyme responsible for degradation of endogenous oleamide and anandamide*, Proc. Natl Acad. Sci. USA 97 (2000), pp. 5044–5049.
[20] K. Ahn, D.S. Johnson, L.R. Fitzgerald, M. Liimatta, A. Arendsen, T. Stevenson, E.T. Lund, R.A. Nugent, T.K. Nomanbhoy, J.P. Alexander, and B.F. Cravatt, *Novel mechanistic class of fatty acid amide hydrolase inhibitors with remarkable selectivity*, Biochemistry 46 (2007), pp. 13019–13030.
[21] M. Mileni, D.S. Johnson, Z. Wang, D.S. Everdeen, M. Liimatta, B. Pabst, K. Bhattacharya, R.A. Nugent, S. Kamtekar, B.F. Cravatt, K. Ahn, and R.C. Stevens, *Structrue-guided inhibitor design for human FAAH by interspecies active site conversion*, Proc. Natl Acad. Sci. USA 105 (2008), pp. 12820–12824.
[22] Q.C. Zheng, Z.S. Li, M. Sun, Y. Zhang, and C.C. Sun, *Homology modeling and substrate binding study of nudix hydrolase Ndx1 from thermos thermophilus HB8*, Biochem. Biophys. Res. Commun. 333 (2005), pp. 881–887.
[23] W. Xu, P. Cai, M. Yan, L. Xu, and P.K. Ouyang, *Molecular docking of xylitol and xylose isomerase from thermus thermophilus and model analysis*, Chem. J. Chinese Universities 28 (2007), pp. 971–973.
[24] Y.P. He, H.R. Hu, and L.S. Xu, *Structure–activity relationship studies on 6-naphthylmethyl substituted HEPT derivatives as non-nucleoside reverse transcriptase inhibitors based on molecular docking*, Chem. J. Chinese Universities 26 (2005), pp. 254–258.
[25] M.H. Bracey, M.A. Hanson, K.R. Masuda, R.C. Stevens, and B.F. Cravatt, *Structural adaptations in a membrane enzyme that terminates endocannabinoid signaling*, Science 298 (2002), pp. 1793–1796.
[26] A. Bairoch and R. Apweiler, *The SWISS-PORT protein sequence data bank and its supplement TrEMBL*, Nucl. Acids Res. 25 (1997), pp. 31–36.
[27] S.F. Altschul, T.L. Madden, A.A. Schfer, J.Z. Zhang, W. Miller, and D.J. Lipman, *Gapped BLAST and PSI-BLAST: a new generation of protein database search programs*, Nucl. Acid. Res. 25 (1997), pp. 3389–3402.
[28] A. Sali and J.P. Overington, *Derivation of rules for comparative protein modeling from a database of protein structure alignments*, Protein Sci. 3 (1994), pp. 1582–1596.
[29] A. Sali and T.L. Blundell, *Comparative protein modeling by satisfaction of spatial restraints*, J. Mol. Biol. 234 (1993), pp. 779–815.
[30] A. Sali, L. Potterton, F. Yuan, H. Vlijmen, and M. Karplus, *Evaluation of comparative protein modeling by modeller*, Proteins 23 (1995), pp. 318–326.
[31] A. Sali and T.L. Blundell, *Definition of general topological equivalence in protein structures. A procedure involving comparison of properties and relationships through simulated annealing and dynamic programming*, Curr. Opin. Biotechnol. 6 (1995), pp. 437–451.
[32] D.A. Case, T.E. Cheatham, III, T. Darden, H. Gohlke, R. Luo, K.M. Merz, A. Onufriew, Jr, C. Simmerling, B. Wang, and R.J. Woods, *The Amber bimolecular simulation programs*, J. Comp. Chem. 26 (2005), pp. 1668–1688.
[33] W.L. Jorgensen, J. Chandraskhar, J. Madura, and M.L. Klein, *Comparison of simple potential functions for simulating liquid water*, J. Chem. Phys. 79 (1983), pp. 926–935.
[34] J.P. Rychaert, G. Ciccotti, and H.J.C. Berendsen, *Numerical integration of the Cartesian equations of motion of a system with constraints: molecular dynamics of* n*-alkanes*, J. Comp. Phys. 23 (1977), pp. 327–341.
[35] Y. Duan, C. Wu, S. Chowdhury, M.C. Lee, G.M. Xiong, W. Zhang, R. Yang, P. Cieplak, R. Luo, T. Lee, J. Caldwell, J. Wang, and P. Kollman, *A point-charge force field for molecular mechanics simulations of proteins based on condensed-phase quantum mechanical calculations*, J. Comp. Chem. 24 (2003), pp. 1999–2012.
[36] *Insight II Profile-3D User Guide*, Biosym/MSI, San Diego, 2000.
[37] R.A. Laskowski, M.W. MacArthur, D.S. Moss, and J.M. Thornton, *PROCHECK: a program to check the stereochemical quality of protein structures*, J. Appl. Cryst. 26 (1993), pp. 283–291.
[38] M.J. Sippl, *Recognition of errors in three-dimensional structures of proteins*, Proteins 17 (1993), pp. 355–362.
[39] *Binding Site Analysis User Guide*, Accelrys Inc., San Diego, CA, USA, 2000.
[40] *Insight II Affinity User Guide*, San Diego, Biosym/MSI, 2000.
[41] M.J.T. Frisch, G.W. Schlegel, H.B. Scuseria, G.E. Robb, M.A. Cheeseman, J.R. Montgomery, Jr, J.A. Vreven, T. Kudin, K.N. Burant, J.C. Millam, G.E. Scuseria, M.A. Robb, J.R. Cheeseman, J.A. Montgomery, Jr., T. Vreven, K.N. Kudin, J.C. Burant, J.M. Millam, S.S. Iyenger, J. Tomasi, V. Barone, B. Mennucci, M. Cossi, G. Scalmani, N. Rega, G.A. Peterson, H. Nakatsuji, M. Hada, M. Ehara, K. Toyota, R. Fukuda, J. Hasegawa, M. Ishida, T. Nakajima, Y. Honda, K. Kitato, N. Nakai, M. Klene, X. Li, J.E. Knox, H.P. Hratchian, J.B. Cross, V. Bakken, C. Adamo, J. Jaramillo, R. Gomperts, R.E. Stratmann, O. Yazyev, A.J. Austin, R. Cammi, C. Pomelli, J.W. Ochterski, P.Y. Ayala, K. Morokuma, G.A. Voth, P. Salvador, J.J. Dannenberg, V.G. Zakrzewski, S. Dapprich, A.D. Daniels, M.C.. Strain, O. Farkas, D.K. Malick, A.D. Rabuck, K. Raghavachari, J.B. Foresman, J.V. Ortiz, Q. Cui, A.G. Baboul, S. Clifford, J. Cioslowski, B.B. Stefanov, G. Liu, A. Liashenko, P. Piskorz, I. Komaromi, R.L. Martin, D.J. Fox, T. Keith, M.A. Al-Laham, C.Y. Peng, A. Nanayakkara, M. Chellacombe, P.M.W. Gill, B. Johnson, W. Chen, M.W. Wong, C. Gonzalez, and J.A. Pople, *Gaussian 03*, Gaussian Inc., Wallingford, CT, 2004.
[42] *Insight II Ludi User Guide*, San Diego, Biosym/MSI, 2000.
[43] D.G. Deutch, S. Lin, W.A. Hill, K.L. Morse, D. Salehani, G. Arreaza, R.L. Omeir, and A. Makriyannis, *Fatty acid sulfonyl fluorides inhibit anandamide metabolism and bind to the cannabinoid receptor*, Biochem. Biophys. Res. Commun. 231 (1997), pp. 217–221.
[44] Y. Segall, G.B. Quistad, D.K. Nomura, and J.E. Casida, *Arachidonylsulfonyl derivatives as cannabinoid CB1 receptor and fatty acid amide hydrolase inhibitors*, Bioorg. Med. Chem. Lett. 13 (2003), pp. 3301–3303.
[45] D.G. Deutch, R. Omeir, G. Arreaza, D. Salehani, G.D. Prestwich, Z. Huang, and A. Howlett, *Methyl arachidonyl fluorophosphonate: a potent irreversible inhibitor of anandamide amidase*, Biochem. Pharmacol. 53 (1997), pp. 255–260.
[46] B. Koutek, G.D. Prestwich, A.C. Howlett, S.A. Chin, D. Salehani, N. Akhavan, and D.G. Deutch, *Inhibitors of arachidonoyl ethanolamide hydrolysis*, J. Biol. Chem. 269 (1994), pp. 22937–22940.
[47] L. De Petrocellis, D. Melck, N. Ueda, S. Maurelli, Y. Kurahashi, S. Yamamoto, G. Marino, and V. Di Marzo, *Novel inhibitors of brain, neuronal, and basophilic anandamide amidohydrolase*, Biochem. Biophys. Res. Commun. 231 (1997), pp. 82–88.
[48] A.H. Lichtman, D. Leung, C. Shelton, A. Saghatelian, C. Hardouin, D.L. Boger, and B.F. Cravatt, *Reversible inhibitors of fatty acid amide hydrolase that promote analgesia: evidence for an unprecented combination of potency and selectivity*, J. Pharmacol. Exp. Ther. 311 (2004), pp. 441–448.
[49] M.J. Myllymäki, S.M. Saario, A.O. Kataja, J.A. Castillo-Melendez, T. Nevalainen, R.O. Juvonen, T. Järvinen, and A.M.P. Koskinen, *Design, synthesis, and in vitro evaluation of carbamate erivatives of 2-benzoxazolyl- and 2-benzothiazolyl-(3-hydroxyphenyl)-methanones as novel fatty acid amide hydrolase inhibitors*, J. Med. Chem. 50 (2007), pp. 4236–4242.
[50] S.-Y. Sit and K. Xie, *WO Patent 087569,* 2002.
[51] S. Patel, E.R. Wohlfeil, D.J. Rademacher, E.J. Carrier, L.J. Perry, A. Kundu, J.R. Falck, K. Nithipatikom, W.B. Campbell, and C.J. Hillard, *The general anesthetic propofol increases brain N-arachidonylethanolamine (anandamide) content and inhibits fatty acid amide hydrolase*, Br. J. Pharmacol. 139 (2003), pp. 1005–1013.
[52] M. Seierstad and J.G. Breitenbucher, *Discovery and development of fatty acid amide hydrolase (FAAH) inhibitors*, J. Med. Chem. 51 (2008), pp. 7327–7343.